Modelling the arching effect in active earth pressure problems

Caroline Thomas and Jim Shiau
Faculty of Engineering & Surveying, University of Southern Queensland, Toowoomba, QLD, Australia

Keywords: stability, earth pressure, gravity wall, numerical analysis, finite difference

ABSTRACT

This paper uses FLAC to analyse the active earth pressure problem. The model used is a rigid gravity retaining wall, with Mohr Coulomb soil backfill and a zero thickness interface element between the wall and backfill to model the sliding and separation between the wall and the backfill soil. Active failure of the soil backfill was induced through pushing the rigid wall away from the backfill, resulting in generation of an ultimate failure load. The results for this paper were compared with the available solutions of similar studies, and major problems encountered during the model development process were discussed.

1. INTRODUCTION

Retaining walls have been examined numerous times by engineers using various approaches such as limit equilibrium, slip line, and limit analyses. As a result of these previous investigations there is a large body of work available to be resourced for informative purposes. Comparatively few investigations, however, have studied the arching effect through the development of numerical models using computer software such as FLAC, the software used in this investigation.

FLAC is a two-dimensional explicit finite difference code used by engineers in both the research and design of a variety of geotechnical structures. FLAC may be used to model the behaviour of rock, soil, or other materials 'that behave plastically when their yield limits are reached' (Itasca 2002). Amongst other situations, the program can model interface elements, groundwater and consolidation, and simulate structural support. In this paper, FLAC is used to investigate active earth pressure on a retaining wall. The investigation both validates and analyses the model through comparison with existing results, as well as providing an insight into possible problems an engineer could encounter when developing numerical models in similar situations. Significant experience is required to thoroughly understand the use of FLAC and its results. Due to this, care was taken when interpreting results to ensure that the model was first behaving correctly, and that the numerical output was correct before considering a program to be a valid representation of the situation.

2. STATEMENT OF THE PROBLEM AND FLAC MODEL DEVELOPMENT

This investigation centres on a retaining wall with a smooth vertical back, cohesionless backfill with no surface surcharge and no standing water behind the backfill. The aim is to determine values of the active earth pressure coefficient $K'_{a\gamma}$, which may be defined as the 'ratio between normal component of earth pressure of a cohesionless mass on a plane surface and the corresponding liquid pressure, if pressure distribution is hydrostatic' (Terzaghi 1966).

In this study the retaining wall was loaded until the active earth pressure condition was created using a small imposed velocity, pushing the wall away from the soil backfill. From this, the load required to create the active state was used to calculate $K'_{a\gamma}$. The failure load was determined using the FLAC 'solve' facility, which solves the problem through the reduction of the nodal unbalanced force. Care was taken to ensure that sufficient movement of the retaining wall occurred to develop the active condition.

As for this investigation the soil was modelled as cohesionless with no surcharge, the equation required to calculate $K'_{a\gamma}$ was effectively the same as in Rankine's Theory. Coulomb theorised, however, that the resultant force on the wall is inclined at an angle δ from perpendicular to the wall where δ is the angle of friction between the wall and the soil (Coduto 1999). Using this information, the active load derived from the FLAC model was divided by $\cos\delta$ to determine the inclined load, and from there calculate the adjusted active earth pressure coefficient.

A plot of the model mesh is shown in Figure 1. Note that the failure wedge for active failure does not extend as far into the backfill as in the passive case, and as such a reduction in model length may be a viable option. In order to model the friction and separation between the retaining wall and the soil backfill, an interface of zero thickness was inserted between the two materials. Wall friction was modelled through alteration of the angle of friction δ and angle of dilation ψ within the interface. For example, when modelling a smooth wall, the angle of friction within the interface may be set at zero degrees, whereas if a perfectly rough wall was desired, the interface friction angle would be adjusted to be equivalent to the angle of friction (i.e. $\delta = \phi$).

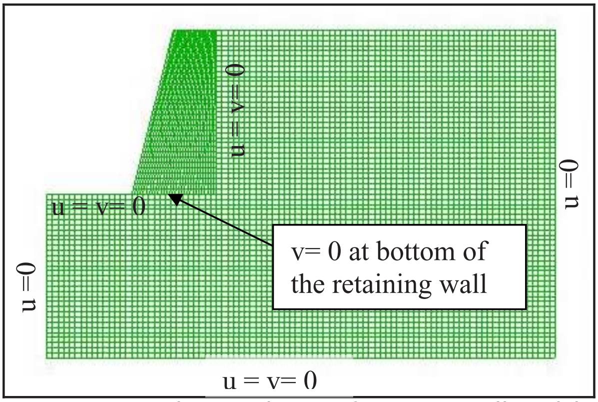

Figure 1: Boundary conditions of retaining wall model

To ensure that the model's boundary conditions were an accurate representation of classic solutions the base of the retaining wall was fixed in the Y direction, simulating a heavy gravity retaining wall (Shiau & Smith 2006), and the soil backfill surface was modelled as 'free' for natural movement.

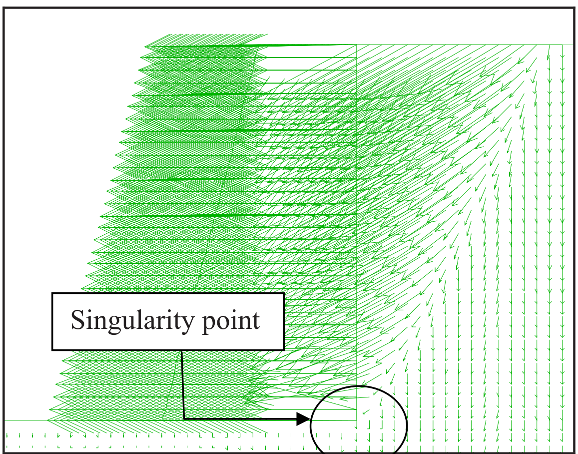

Figure 2: Displacement plot for active failure

3. **RESULTS AND DISCUSSIONS**

A typical plot of velocity field is shown in Figure 2. The major problem with the analysis arose due to a singularity point occurring at the lower right hand corner of the retaining wall. The cause of this instability is essentially elements around the corner of the retaining wall subjected to tension and compression simultaneously, which is numerically infeasible. This indirectly indicates velocity discontinuity (or element separation) around the corner point (Figures 2 and 3) and therefore a discontinuous model, that allows element separation, is preferred to solve this problem (Lyamin and Sloan, 2003).

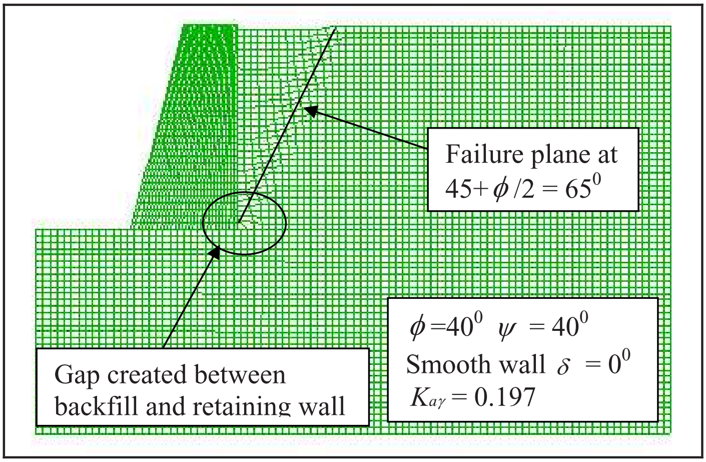

Figure 3: Exaggerated grid distortion of retaining wall model at active failure condition

Figure 3 shows a typical magnified grid distortion of the retaining wall backfill at active failure. Also visible from Figure 3 is a gap created between the retaining wall and the soil backfill as the wall moves away from the soil. It appears to be the result of the elements at the very corner of the soil backfill remaining stationary as the failure wedge above slides along the plane into the gap created as the wall moves away, which in reality would cause a very small gap. The presence of the gap was confirmed by altering the fixity around this corner to determine the most realistic soil movement. Note that the presence of this gap influences the pressure distribution (discussed later in this section) and results in a reaction force of zero at the bottom element which will in turn decrease the value of the active earth pressure coefficient $K_{a\gamma}$.

Figure 4 plots the contours of maximum shear strain rate. Note that there is a notable peak in the shear strain rate around the corner point of the retaining wall.

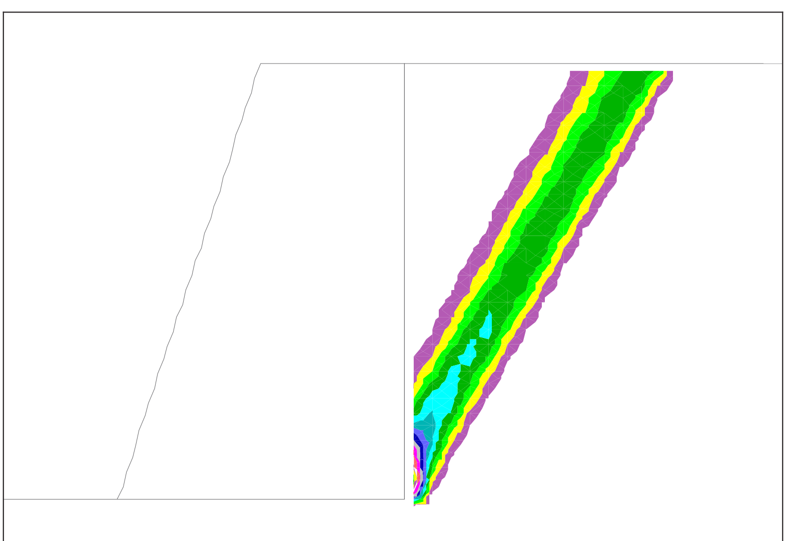

Figure 4: Contours of maximum shear strain rate for a smooth wall
($\phi=40^0$, $\delta = 0^0$, $\psi = 40^0$)

3.1 Arching effect

Observation of the deformation of the soil backfill reveals the presence of the phenomenon of soil arching (Figure 3). Terzaghi (1943) investigated this effect and described it as the 'transfer of pressure from a yielding mass of soil onto adjoining stationary parts.' Terzaghi preferred to qualitatively define the situation and never actually drew an arch. Later investigation by Handy (1983) revealed a flat arch such as that shown in Figure 5. Coduto (1999) mentioned that in reality the pressure distribution behind retaining wall is not triangular, but rather is concave, and this is a reflection of 'wall deflections, arching and other factors'. This figure illustrates the substantial difference between the two types of pressure distributions. The logical result of this difference between the distributions is the inference that Coulomb's theorem overestimates the active earth pressure. More recent investigation by Harrop-Williams (1989) was able to determine an equation for this distribution, though analysis of this equation was not within the scope of this investigation.

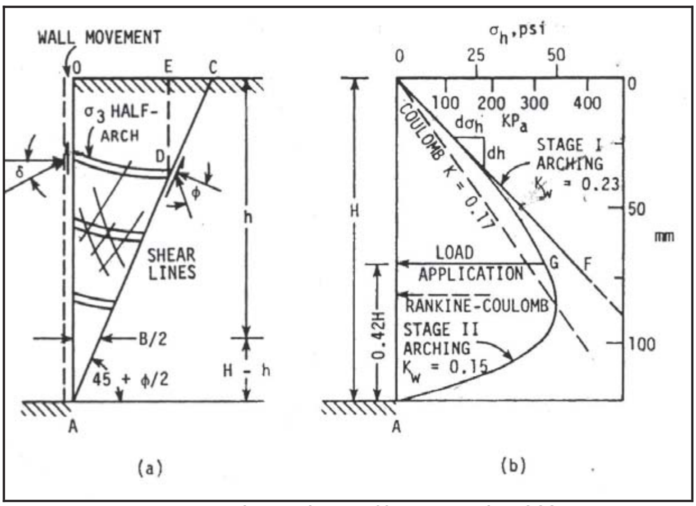

Figure 5: The arching effect (Handy 1983)

This investigation has also discovered that the pressure distribution behind the retaining wall is non-linear. Figure 6 plots the reaction forces along one side of the interface between the retaining wall and the soil backfill. The plot shows a clear concave distribution, compatible to Handy's (1983) investigations. In addition to this the figure illustrates the lack of stress on the bottom elements, which is a result of the gap in the soil backfill at failure discussed above.

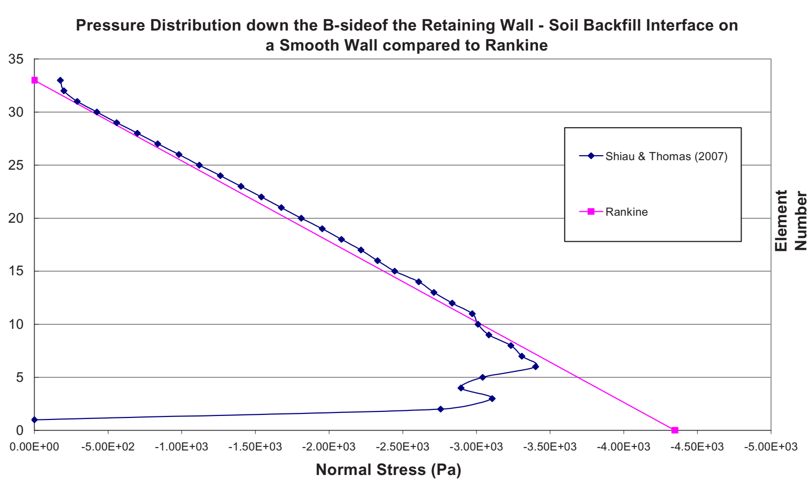

Figure 6: Concave pressure distribution

Figure 7 demonstrates the sagging that occurs in the elements within the failure plane at the active earth pressure condition. This finding is in agreement with the findings of Handy (1983). The arching effect is clearly present in the moving elements between the interface and the stationary elements. In this figure, the solid lines are representative of the model's undeformed condition whilst the dotted lines are indicative of the position the elements would be in at the active condition. This is an exaggerated plot of the active condition.

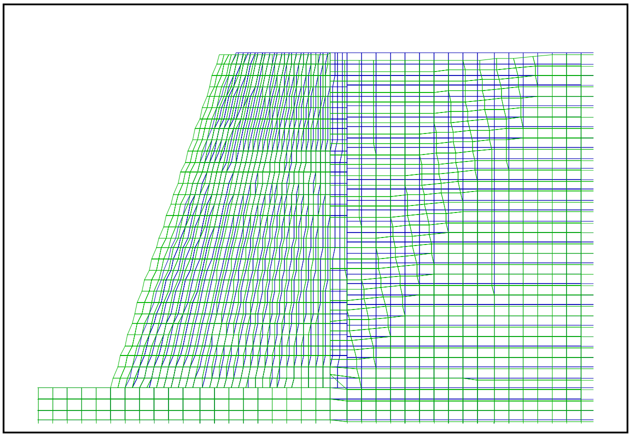

Figure 7: Sagging in the retaining wall backfill at active condition

3.2 Associate/Non-associate conditions

Associated flow refers to the restriction of plastic flow such that the dilation angle is equivalent to the soil friction angle (i.e. $\psi = \phi$). In reality, however, the dilation angle is always smaller than the angle of friction ($\psi < \phi$) (Shiau and Smith 2006). The traditional analysis using the limit equilibrium theory assumes associated flow rule, and the study presented above is for associated flow conditions. The following graphs show the influence of dilation angle on maximum shear strain rate and the active earth pressure coefficient, $K_{a\gamma}$.

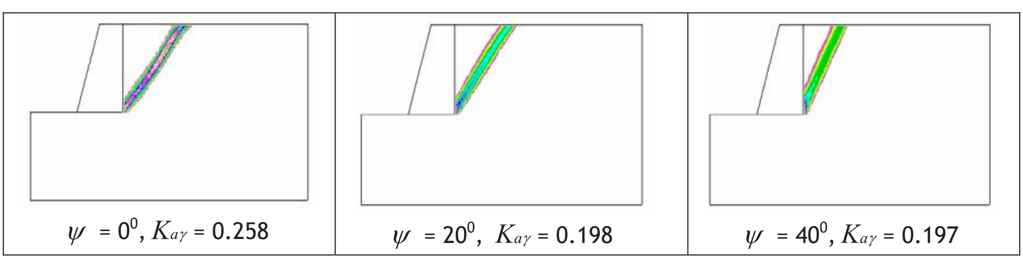

Figure 8: Variation in maximum shear strain rate and $K_{a\gamma}$ for various wall friction angles δ and dilation angles ψ when angle of friction is 40^0 (smooth wall).

Evidently, changing dilation angle when the angle of friction is fixed does have an impact on the distribution of maximum shear strain rate. Note that decreasing the dilation angles increases the active earth pressure coefficient $K_{a\gamma}$. For associative conditions, where $\psi = \phi$ FLAC returned a $K_{a\gamma}$ of 0.197. Realistically, however, the dilation angle will be between zero degrees and the angle of friction ϕ. Therefore, these diagrams show that the assumption of associated flow conditions in the traditional method of retaining wall design may result in an underestimation of the active earth pressure coefficient $K_{a\gamma}$, and the resultant active earth pressure.

4. CONCLUSIONS

This investigation has been successful in using FLAC software to model the active earth pressure condition of a gravity retaining wall. Problems occurring within the model development process were mainly caused by a singular point at the lower right-hand corner of the retaining wall, which resulted in a stress peak and illogical movement of the soil about this point. A number of methods were investigated that could potentially limit the influence of this problem, but the most effective method for this case was determined to be a simple decrease in the size of the elements across the entire mesh, which resulted in a drastic improvement in the stress peak at the corner of the retaining wall, as well as in the movement of the soil about this corner.

Also investigated was the presence of an 'arching effect' and the effect of non-associate flow rule during plastic shearing. Analysis of the soil behaviour in response to changing dilation angles concluded that the assumption of associated flow conditions in the traditional method of retaining wall design may result in an underestimation of the active earth pressure coefficient $K_{a\gamma}$, and the resultant active earth pressure. Further study of 3D arching effects shall be carried out in the future.

ACKNOWLEDGEMENTS

The authors would like to thank Catherine Smith for her thoughtful and thorough proof reading of this paper.

REFERENCES

Coduto, DP (1999), *Geotechnical Engineering Principles and Practices,* Horton, M. & De Leon. L.M. (eds.), Prentice Hall, Sydney.

Handy, RL (1983), 'The Arch in Soil Arching', *Journal of Geotechnical Engineering,* ASCE, Vol. 111, No.3.

Harrop-Williams, KO (1989), 'Geostatic Wall Pressures', *Journal of Geotechnical Engineering*, ASCE, Vol. 115, No. 9.

Itasca Consulting Group (2002), *FLAC Fast Lagrangian Analysis of Continua User's Guide*, Itasca, USA.

Lyamin, A. V. and Sloan, S. W. (2002). 'Lower Bound Limit Analysis using Non-linear Programming', *International Journal for Numerical Methods in Engineering*, 55, 573-611.

Shiau, JS and Smith, CA (2006), 'Numerical Analysis of Passive Earth Pressures with Interfaces', Paper presented to III European Conference on Computation Mechanics, Portugal, 5-8 June.

Shiau, JS, Lyamin, AV and Sloan, SW (2006), 'Determination of Active and Passive Earth Pressure Coefficients using Rigorous Limit Analyses', *Canadian Geotechnical Journal* (to submit).

Terzaghi, K (1966), *Theoretical Soil Mechanics,* John Wiley and Sons, New York.

Van Langden, H and Vermeer, PA (1991), 'Interface Elements for Singular Plasticity Points', *International Journal for Numerical and Analytical Methods in Geomechanics,* Vol 15, pp. 301-305.